Neural Network-Based Multi-DOA Tracking for High Speed Railway Communication Systems

Yu Zheng, Yue Xiao, Zheng Ma, *Member, IEEE,* Panagiotis D.Diamantoulakis, *Senior Member, IEEE,* George K. Karagiannidis, *Fellow, IEEE,*

***Abstract*—Along with the rapid development of high-speed railway (HSR), it is of vital importance to explore new technologies to meet the stringent requirements on wireless transmission latency and reliability in such high mobility scenarios. To address this, fast beamforming schemes with precise direction-of-arrival (DOA) can achieve effective channel gain and improve interference mitigation. In this paper, we propose a novel radial-basis function neural network (RBFNN)-based method for the multi-DOA tracking, in which the RBFNN is trained by the location-based prior information. Consequently, the DOA tracking problem is transformed into an RBFNN with trained input/output pairs. The effectiveness of the proposed scheme in terms of complexity and accuracy is verified by simulation results. Finally, the impact of the shapes of the array on estimation accuracy is also discussed.**

***Index Terms*—high-speed railway (HSR), DOAs (direction-of-arrivals) tracking, radial-basis function neural network (RBFNN).**

I. Introduction

In the railway wireless communication systems (RWCS), the interference is a severe problem, which imposes a serious threat to the safety of train operations. However, in the high-speed railway (HSR) scenario, the rapid and drastic changes in both wireless channels and direction-of-arrivals (DOAs) make the traditional DOA estimation-based beamforming inefficient to mitigate the interference [1]. Specifically, traditional DOA estimation algorithms are generally based on subspace tracking, such as multiple signal classification (MUSIC), estimating signal parameter via rotational invariance techniques (ESPRIT), projection approximate space tracking (PAST) algorithm, and projection approximate space tracking with deflation (PASTd) algorithm [2]-[4], etc. The common feature of these algorithms is based on eigenvalue composition, which causes a high calculation overhead. As a result, it is difficult to be implemented in real-time to track the rapid changes of DOAs. Obviously, these algorithms are not suitable for HSR scene.

In order to meet the requirements of high accuracy and real-time calculation, the use of artificial neural networks for DOA estimation algorithms was proposed and investigated in [5]-[10]. One of the main advantages of neural networks is that they can be implemented by analog circuits, and computation time can reach the nanosecond level [5], [7]. However, the previous neural network-enabled methods for DOA tracking are mainly based on blind detection, by feeding with extremely huge data sets. Similarly, the need for a large amount of data sets still makes it difficult to be deployed in practical implementation for RWCS. Nevertheless, the prior information of HSR, such as the regularity of moving direction and route, the availability of speed and position, brings new opportunities to the application of the neural network for RWCS. To the best of our knowledge, no work has been devoted to achieving real-time DOA tracking in RWCS.

Based on the above discussion, this paper proposes an efficient location-based RBFNN for multi-DOA tracking in RWCS to overcome the redundant time consumed for communication in the blind detection-based method [8]. By incorporating the prior knowledge of the train's location into the neural network based DOA tracking algorithm framework, the investigated train only needs to collect limited data sets from a fixed number of base stations (BSs) along the rail track, by which more exact and lower volume of training samples are constructed. Thus the proposed scheme can be implemented to meet the requirement of low transmission latency and high reliability in RWCS. Simulation results prove the superiority of this real-time processing method.

The rest of the paper is organized as follows. Section II establishes the DOA model for the RWCS. In Section III, a novel RBFNN for location-based multi-DOA tracking is illustrated. Section IV analyses the time complexity of both the proposed and subspace tracking methods. Simulation results are carried out and discussed in Section V followed by the conclusion in Section VI.

II. Direction of Arrival Modeling

Considering an RWCS as shown in Fig. 1, a train simultaneously receives the desired signal from its serving cell and interference signals from neighboring cells. For ease of description, we assume that the train travels in the environment with no reflections and scatters, such as plain and viaduct, which is also in accord with the most common scenario in HSR system [11]. Therefore, the communication links between BSs and vehicle-mounted antennas are regarded as a line of sight (LOS) [12]. Thus, it is reasonable to assume that the angel shifts in this HSR scene are too small to be ignored. Moreover, it is assumed that accurate speed and position information of the train can be obtained in RWCS, then the Doppler shift of the train can be effectively compensated at any time, i.e. there are no Doppler effects considered in the following work.

Corresponding authors: Zheng Ma, Yue Xiao.

Y. Zheng, Y. Xiao, and Z. Ma are with the Provincial Key Lab of Information Coding and Transmission, Southwest Jiaotong University, Chengdu 611756, China (e-mails: zhengyu@my.swjtu.edu.cn; alice_xiaoyue@hotmail.com; zma@swjtu.cn).

Panagiotis D.Diamantoulakis and G. K. Karagiannidis are with the Provincial Key Laboratory of Information Coding and Transmission, Southwest Jiaotong University, Chengdu 610031, China, and also with the Electrical and Computer Engineering Department, Aristotle University of Thessaloniki, 54124 Thessaloniki, Greece (e-mail: padiaman@auth.gr; geokarag@auth.gr).

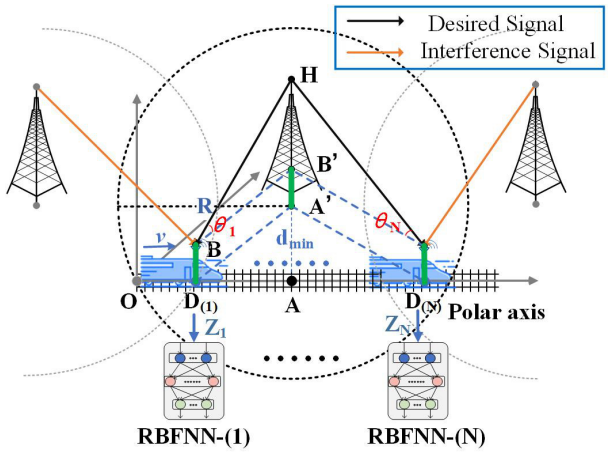

Fig. 1. System model of HSR for DOA tracking.

A. Direction of Arrival Calculation

For the sake of description, the polar coordinate system is utilized to depict positions of all participated devices, with the projection of the train (initial position) at the ground' plane as the reference point (denoted by O), as shown in Fig.1. H and B denote the top of the antenna mounted on the BS and the train, respectively. Moreover, we let A′ as the foot of the BS, which is also viewed as the center of a cell, thus we have the cellular radius as $\mathrm{OA}' = \mathrm{r}$, then the height of the BS can be given by $\mathrm{HA}' = h_{\mathrm{t}}$. Moreover, we denote A and D as the projection of the point A′ and B on the railway track, respectively. Herein, there are $\mathrm{AA}' = \mathrm{d_{min}}$, $\mathrm{OA} = \mathrm{d_{OA}}$, $\mathrm{AD} = \mathrm{d_{AD}}$, $\mathrm{A'D} = \mathrm{d_{A'D}}$. To establish the DOA calculation in one space, an auxiliary point B′ is added on the body of the BS to satisfy that $\mathrm{BD} = \mathrm{A'B'} = h_{\mathrm{r}}$. In addition, we assume the speed of the train is v. Thus, the function of the DOA of the train at time-t $\theta(t)$ can be deduced as

$$d_{\mathrm{OA}} = \sqrt{r^2 - d_{\mathrm{min}}^2}, \tag{1}$$

$$d_{\mathrm{AD}}(t) = |d_{\mathrm{OA}} - vt|, \tag{2}$$

$$d_{\mathrm{A'D}}(t) = \sqrt{d_{\mathrm{AD}}(t)^2 + d_{\mathrm{min}}^2}, \tag{3}$$

$$\theta(t) = \angle \mathrm{HBB}' = \arctan \frac{h_{\mathrm{t}} - h_{\mathrm{r}}}{d_{\mathrm{A'D}}(t)}, \tag{4}$$

where $0 \leq t < \frac{2d_{\mathrm{OA}}}{v}$. Obviously, we can easily derive the nonlinear DOA function of the interference signals in the same way. For simplicity, DOAs of the interference signals are supposed as linear functions hereinafter.

B. Direction of Arrival Mapping Procedure

In what follows, we establish the standard model of DOA estimation [2]-[4], [6]-[8]. The narrowband signals $S(t) = [s_1(t), s_2(t), ...s_K(t)]^{\mathbf{T}}$ with the carrier frequency being equal to f_0 are incident on a linear array with $M(K < M)$ elements from K directions $\Theta = [\theta_1, \theta_2, ...\theta_K]^{\mathbf{T}}$, which include desired and interference directions. Notably, the train is expected to receive the fixed K signals from BSs along the rail track. Thus, the array manifold can be defined as a $M \times K$ steering matrix given as

$$\mathbf{A} = [\alpha(\theta_1), \alpha(\theta_2), ...\alpha(\theta_K)], \tag{5}$$

where $\alpha(\theta_k) = [1 \ e^{-j\omega} \ e^{-j2\omega} \ ... \ e^{-j(M-1)\omega}]^{\mathrm{T}}$, $\omega = \frac{2\pi f_0 d}{c} \sin\theta_k$. Moreover, d is the spacing between the neighboring elements of the array, c is the speed of light in free space. The received signals incident on the array output can be expressed as

$$\begin{aligned} \mathbf{X}(t) &= \sum_{k=1}^{K} \alpha(\theta_k) s_k(t) + \mathbf{N}(t) \\ &= \mathbf{A}\mathbf{S}(t) + \mathbf{N}(t), \end{aligned} \tag{6}$$

where $t \in [1, T]$, with T being the total number of collected snapshots. $\mathbf{S}(t)$ represents the incident signals. $\mathbf{N}(t)$ denotes the statistically independent white noise signal with zero mean and variance σ^2, which is also independent of $\mathbf{S}(t)$. Then, the covariance matrix containing spatial orientation information can be expressed as

$$\mathbf{R}_{xx} = \mathbf{E}[\mathbf{X}(t)\mathbf{X}(t)^{\mathbf{H}}] = \begin{bmatrix} \mathbf{r}_{1,1} & \mathbf{r}_{1,2} & \cdots & \mathbf{r}_{1,M} \\ \mathbf{r}_{2,1} & \mathbf{r}_{2,2} & \cdots & \mathbf{r}_{2,M} \\ \vdots & \vdots & \ddots & \vdots \\ \mathbf{r}_{M,1} & \mathbf{r}_{M,2} & \cdots & \mathbf{r}_{M,M} \end{bmatrix}. \tag{7}$$

Thus, the mapping from DOAs $\Theta = [\theta_1, \theta_2, ...\theta_K]^{\mathbf{T}}$ to the array output $\mathbf{X} = [x_1(t), x_2(t), ..., x_M(t)]^{\mathbf{T}}$ is described as $G : \Psi^K \rightarrow \Omega^M$. DOAs tracking problem is equivalent to the inverse mapping $F : \Omega^M \rightarrow \Psi^K$ [8].

III. Location Information Based Neural Network For Multiple DoA Tracking

Due to the high mobility of the HSR scene, i.e., the average speed of the high-speed train can be around 350-km/h [1], significant angle offsets and excessive feedback delay for signals are inevitable when leveraging the conventional signal processing techniques [2]-[4], thus resulting in large estimation error of channel-state related information. Based on the above discussion, the location-inspired neural network for the multi-DOA tracking mechanism is proposed in this section. Specifically, a simple three-layer feed-forward network, i.e., the RBFNN is leveraged, to satisfy the low-latency requirement for the practical HSR wireless networks, benefits from its low complexity and fast training speed compared with other multi-layer neural networks counterparts. It is noteworthy that in the practical implementations of the HSR scene, the trial operation stage of the high-speed train is vital before entering the official operation, which introduces a good platform for the off-line training of the learning model. To this end, the trained RBFNN model can be utilized to evaluate the actual DOA estimation, during the official operation.

A. Data Preprocessing for Neural Networks

In general, the M^2-dimensional matrix $\mathbf{R}_{xx}$, which contains sufficient information about DOAs, is reformed as a column vector as the input of the neural network. However, it is better for us to reduce the dimension of the input vector, because the lower scale of neural networks means the lower latency. Considering both computation and accuracy of the neural network, we use the preprocessing schemes in [8]. Based on that, by utilizing the symmetry of the correlation matrix, we

only need to reorganize the upper or lower triangular part of the matrix $\mathbf{R}_{xx}$ (7) as an $\frac{1}{2}M(M+1)$-dimensional input vector $\mathbf{b}$ given by

$$\mathbf{b} = [\mathbf{r}_{1,1}, \cdots, \mathbf{r}_{1,M}, \mathbf{r}_{2,2}, \cdots, \mathbf{r}_{2,M}, \cdots, \mathbf{r}_{M,M}]. \quad (8)$$

Since the neural network can't deal with complex numbers directly [8], the real and imaginary parts of each element in the vector $\mathbf{b}$ should be recombined into an $M(M+1)$-dimensional vector $\mathbf{B}$ expressed as

$$\mathbf{B} = [\mathrm{Re}(\mathrm{vec}(\mathbf{b})), \mathrm{Im}(\mathrm{vec}(\mathbf{b}))] \in \mathbb{R}^{M(M+1)}, \quad (9)$$

where $\mathrm{Re}(\cdot)$ and $\mathrm{Im}(\cdot)$ denote the real and imaginary parts respectively. Normalize the vector $\mathbf{B}$ and apply it as the input vector to the neural network expressed as

$$\mathbf{Z} = \frac{\mathbf{B}}{|\mathbf{B}|} = \{\mathbf{z}^{(m)} | m \in (1, \cdots, M(M+1))\}. \quad (10)$$

By doing so, with the redundant or irrelevant information removed, the dimension of the input neural node is reduced from $2M^2$ to $M(M+1)$.

B. Network Training and Testing

As depicted in Fig. 1, N sample locations are set along the railway track and each location corresponds to a RBFNN. Moreover, let assume that the train reaches each tagged location l_n at a certain time t_n, $n \in (1, ..., N)$. With these prior known locations, there is a one-to-one fixed mapping between each different location l_n and the corresponding set of DOAs' combination Θ_{l_n} calculated by the geometry topology established in section II. Thus, for each location-based RBFNN, the set of DOAs' combination from K directions is treated as the label/output of the training/testing set given by

$$\Theta_{l_n}^{(k)} = \{\theta_k(t_n) | k \in (1, \cdots, K)\}. \quad (11)$$

The corresponding input $\mathbf{Z}_{l_n}$ is formed based on the $C-$ point time domain sampled waveform of the array output (6) by utilizing (5)$-$(10). Thus, the input set of the training set can be expressed as

$$\mathbf{Z}_{l_n}^{(c,m)} = \{\mathbf{z}^{(m)}(c) | c \in (1, \cdots, C)\}. \quad (12)$$

After that, the additive Gaussian white noise with mean zero and variance σ_t^2 is added to each element of the training/testing set, which is given by

$$\{\mathbf{Z}_{l_n}^{(c,m)} = \mathcal{CN}(\mathbf{Z}_{l_n}^{(c,m)}, \sigma_t^2) | c \in (1, \cdots, C)\}. \quad (13)$$

Thus, the mapping relationship about each location-based network can be described as $\mathbf{Z}_{l_n}^{(c,m)} \rightarrow \Theta_{l_n}^{(k)}$. The training/testing sets for total number of location-based RBFNNs are written as input/output pairs $\{\mathbf{Z}_{l_n}^{(c,m)}, \Theta_{l_n}^{(k)}\}$. It should be mentioned that these generated data sets are randomly split into training (90%) and testing sets (10%) for training and testing the network respectively. By doing so, the optimal model weights of the RBFNN model can be obtained by using the unsupervised learning algorithm (the K-Means [13]) and the least squares (LS) [14] algorithm. Till now, once the array senses the actual signal, the well-trained RBFNN can get the estimation of DOAs $\hat{\Theta}^{(k)}$ in real-time mapping.

Note that the common assumptions in this paper are the known K fixed roadside BSs and trajectories of the train l_n. Instead of using the extremely huge and coarse grid set for the blind detection method [8], the proposed method only need to train lower volume but more exact training samples. Thus, with lower calculation and smaller storage, the proposed scheme can be implemented to tackle with the practical challenges in RWCS.

IV. Time Complexity Analysis

In this section, we derive the time complexity of the proposed and the subspace tracking methods to demonstrate the real-time processing of both methods in RWCS. Specifically, the conventional subspace tracking method based on PASTD algorithm [4] is chosen as a benchmark for highlighting our proposed scheme. The key idea of this kind of algorithm is that the subspace of the signal at the current moment is approximated by the signal subspace which is prior known at the previous moment. For the stationary or slowly time-varying signal, the projection difference between two adjacent moments is negligible, thus the approximation can be effective. However, the signal projection between two consecutive moments will be quite different due to high mobility in the HSR scenario. In that case, the approximation for subspace tracking may fail. For subspace tracking, we use PASTD algorithm to track the signal subspace in the first stage and choose MUSIC algorithm to estimate DOA in the second stage. The time complexity of subspace tracking is defined as T_{sub}, while T_{pastd} and T_{music} denote the time complexity of PASTD and MUSIC algorithm at each sample point, respectively. C denotes the number of the sample point, K is the number of sources, M is the number of the antenna elements, F denotes the resolution ratio of MUSIC algorithm, and all these paraments can be regarded as constant except C. For each sample point, the computation of PASTD is $4CK + \mathbf{O}(K)$ [4], whereas the computation of MUSIC is $\mathbf{O}(FMK)$. For sequential algorithms, we can approximate their total complexity to the maximum between them. Thus, the time complexity of subspace tracking $T_{\mathrm{sub}}(C)$ is regarded as $C * (\max(T_{\mathrm{pastd}}(C), T_{\mathrm{music}}(C)))$. As a result, the overall time complexity of subspace tracking $T_{\mathrm{sub}}(C)$ is $\mathbf{O}(C^2)$.

TABLE I
Complexity of two method

Algorithm	Complexity
PASTD+MUSIC	$\mathbf{O}(C^2)$
RBFNN	$\mathbf{O}(\frac{P+C}{C})$

For the proposed location-inspired tracking scheme, each location-based RBFNN can be processed in parallel, hence we only need to consider the processing time with one single RBFNN. The time complexity of k-means T_{km} and least squares T_{ls} are $\mathbf{O}(CYL)$ and $\mathbf{O}(LUP)$ respectively, where C is the number of sample points, L is the number of nodes in the hidden layer, Y is the number of nodes in the input layer, U is the number of nodes in the output layer, P is a characteristic dimension of the vector output by k-means algorithm, and all of them can be considered as constant except C and P. Thus, the off-line training time complexity T_{train}, which equals to

$T_{\rm km} + T_{\rm ls}$, can be approximated as: $\mathbf{O}(P + C)$. For the on-line mapping stage, the complexity $T_{\rm map}$ is $\mathbf{O}(L(2M + K))$. Notice that, in general, the time complexity of estimation of on-line mapping $T_{\rm map}$ is an adequate measure for the overall execution time of the proposed scheme, because the RBFNN has already been well-trained by prior information beforehand. However, there is no prior information that could be used to train in subspace tracking, for the fairness of comparison, we should consider the time complexity of off-line training $T_{\rm train}$ as a part of the measurement of the total execution time. Thus the total time complexity of the proposed tracking scheme is

$$T_{\rm neu} = \frac{T_{\rm train}}{C} + T_{\rm map}, \tag{14}$$

where C also represents the maximum training times in the training process. Combined with the above inference, the time complexity of the proposed tracking scheme $T_{\rm neu}$ is $\mathbf{O}(\frac{P+C}{C})$, where P is a variable smaller than C and varies with C. When $C \to \infty$, $\mathbf{O}(\frac{P+C}{C}) \to \mathbf{O}(1)$.

From the comparison of the time complexity, it is obvious that $T_{\rm neu}$ is two orders smaller than $T_{\rm sub}$. Thus, the proposed method has the lower complexity than subspace method.

V. Simulation Results And Discussion

TABLE II
Simulation Parameters

Param	Definition	Values
N	the number of snapshots	1500
R	radius of the cell	6km
v	train velocity	350km/h
f_0	carrier frequency	900MHz
c	speed of light in free-space	$3 \times 10^8 m/s$
$\frac{d}{\lambda}$	ratio of the element spacing to wavelength	0.5
K	the number of sources	3
h_t	antenna height at the BS	80m
h_r	antenna height at the roof of the train	17m
d_{min}	the minimum distance between BS and rail	10m
M	the number of array elements	4, 6, 8, 10, 15
$ArPar$	different array geometry	ULA, UCA, UAA
$SINR$	signal to interference and noise ratio	-10dB,$\cdots$,60dB

In this section, simulation results are provided to demonstrate the performance of the proposed scheme for fast DOA tracking in RWCS. Moreover, to highlight the advantages of the proposed scheme, we also compare the performance between the existing method (including subspace tracking and the blind detection-based method in [8]) and the proposed method. As shown in Fig.1, we only consider three sources $(K = 3)$ including one desire signal of the serving cell and two interference signals from the neighboring cells. Parameters for the simulation are presented in Table II.

A. Performance of the Proposed Method

As shown in Fig. 2(a), the simulation results of the proposed method can fully trace the DOAs change, which implies that the RBFNN has a strong nonlinear fitting capacity even under the high velocity of the high-speed train.

Fig. 2(b) plots the mean square error (MSE) of the DOA estimation versus the number of neurons under the different signal to interference and noise ratio (SINR), and it is shown that with the increasing number of neurons in the hidden layer to 100, the MSE converges rapidly to a stable value, while the MSE decreases with the increase of SINR. It should be mentioned that the number of neurons in hidden layer is usually set to be larger than it of in the input layer while less than the training samples in total for good performance in practical implementation.

In Fig. 2(c), the MSE versus the number of neurons under the different number of array is simulated. It shows that the MSE rapidly reaches a stable value with the neuron number increasing to 100 and the MSE also decreases with the increasing of the antenna elements. Noted that when the number of the antenna elements is 6, 8, and 10, the improvement of performance is not apparent. Hence in consideration of the cost of train operation and the size of the train roof space, one should carefully select the size of antenna for juggling the performance and cost in practical implementation.

Fig. 2(d) plots the performance of MSE under the different array geometry, where six-element UCA (uniform circular array), ULA (uniform linear array) and UAA (uniform arc array) are taken as examples. The simulation results indicate that the performance of UCA is slightly better than that of UAA, while the performance of ULA is the worst. However, ULA is the easiest one to implement in hardware. It should be noticed that the array manifolds of UCA, UAA, and any other nonlinear array geometry are not Vandermonde matrices, which lead to the corresponding correlative matrices of the received signals are not Hermite matrices. Thus, in this simulation, the entire elements of the corresponding correlative matrix $\mathbf{R}_{xx}$ (7) must be used for the input of the network rather than the preprocessed vectors $\mathbf{Z}$ (10), which cause the input size of the neural network increasing from $M(M+1)$ to $2M^2$. Hence the improvement of the MSE performance comes at the expense of complexity with the nonlinear geometry array. Similar with choosing the number of antenna, the reasonable choice of the the array geometry should be taken into consideration for the trade-off between the performance and cost in practical implementation.

B. Comparison of Tracking Accuracy with Subspace Methods

Fig. 3(a) plots the tracking performance of the proposed location-based RBFNN, while Fig. 3(b) performs the tracking performance of the subspace tracking, which we term as the "PASTD+MUSIC" algorithm. Observed from them, the subspace algorithm can not track the nonlinear change of the DOA under the high-speed moving scenario of RWCS, and the results of the estimation are quite different from the theoretical value. Therefore, the subspace tracking method is not applicable in RWCS. By contrast, the proposed location-based RBFNN can fully trace the nonlinear change of the DOA. Thus, our proposed method has the superiority in fast tracking accuracy in practical implementation, which implies that it can tackle the fast DOA tracking in RWCS.

C. Comparison with the Method in [8]

In order to highlight the superiority of the proposed method over that presented in [8], we conduct two experiments to compare the MSE performance and the convergence speed between the two methods in the case of the same training data size in total or per label, respectively. The corresponding

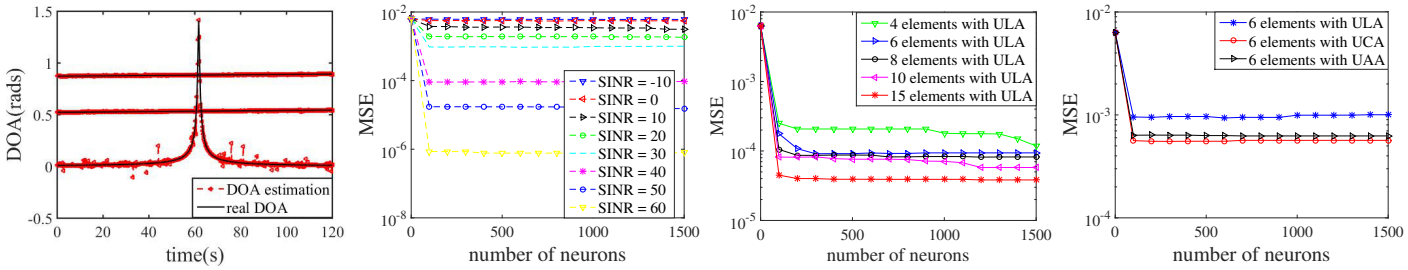

(a) (b) (c) (d)

Fig. 2. (a) Simulation results of the DOAs vs. time in HSR scene. (b) RMSE vs. number of neurons in hidden layer with different SINR. (c) RMSE vs. number of neurons in hidden layer with different number of antenna elements. (d) RMSE vs. number of neurons in hidden layer with different array geometry.

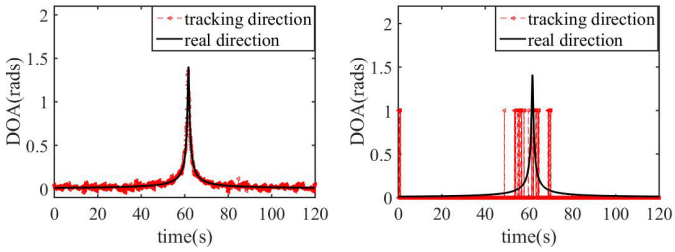

(a) (b)

Fig. 3. (a) DOA vs. time using RBFNN. (b) DOA vs. time using subspace tracking (PASTD+MUSIC).

simulation results are carried out in Fig. 4(a) and Fig. 4(b). Specifically, the value of K is set as 1, for simplification. Moreover, the total training samples is fixed as 600 in Fig. 4(a), while the number of samples per label is set as 200 in Fig. 4(b). Observed from Fig. 4(a), one can figure out that the proposed method has greater accuracy than the blind method [8]. In Fig. 4(b), the convergence of the proposed method at the stable level is faster than the method in [8] does. The MSE performance of the proposed method is also slightly better than the method in [8] in Fig. 4(b). Consequently, the superiority of the proposed method can be conclude as better MSE performance and faster convergence. In particular, this superiority comes from more exact training labels and lower volume of training samples than the method in [8]. More specifically, the extra storage cost by the blind detection method in [8] compared to the proposed scheme, can be denoted as $\sum_{k=1}^{K}\left(\binom{\lfloor\frac{90}{\rho}\rfloor+1}{k}\right)-1$, where ρ is resolution of angle region.

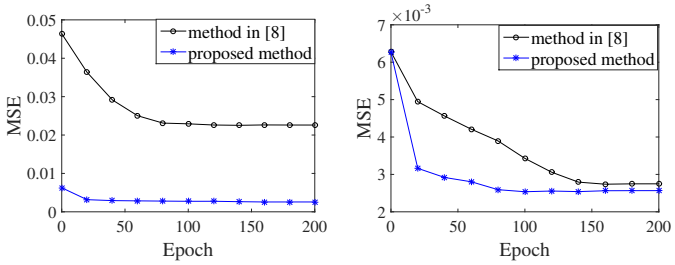

(a) (b)

Fig. 4. Fig 4. (a) MSE vs.Epoch with the same training data size in total. (b) MSE vs. Epoch with the same training data size per label.

VI. Conclusion

In this paper, we investigated multi-DOA tracking in RWCS. We set up the mathematical model of DOAs tracking and proposed a location-based information RBFNN. Simulation results showed that the proposed scheme are very close to the actual desired DOA even when the DOA changes fast and dramatically, while the baseline subspace tracking fails to reach the accuracy as expected. Complexity analysis was also performed to verify the superiority of real-time tracking based on the RBFNN. We also showed the accuracy of the DOA estimation in RWCS is improving with the increase of the number of arrays and the complexity of the array geometry. Moreover, the comparison of the performance to the blind detection method in [8] also showed the superiority of the proposed method.

References

[1] Z. Ma, X. Chen, M. Xiao, G. K. Karagiannidis and P. Fan, "Interference Control for Railway Wireless Communication Systems: Techniques, Challenges and Trends," *IEEE Veh. Technol. Mag.*, vol. 15, no. 3, pp. 51-58, Sept. 2020.

[2] R. Schmidt, "Multiple emitter location and signal parameter estimation," *IEEE Trans. Antennas Propag.*, vol. 34, no. 3, pp. 276-280, Mar. 1986.

[3] R. Roy and T. Kailath, "ESPRIT-estimation of signal parameters via rotational invariance techniques," *IEEE Trans. Acoust., Speech, Signal Process.*, vol. 37, no. 7, pp. 984-995, Jul. 1989.

[4] Bin Yang, "Projection approximation subspace tracking," *IEEE Trans. Signal Process.*, vol. 43, no. 1, pp. 95-107, Jan. 1995.

[5] M. Yang et al., "Machine-Learning-Based Fast Angle-of-Arrival Recognition for Vehicular Communications," *IEEE Trans. Veh. Technol.*, vol. 70, no. 2, pp. 1592-1605, Feb. 2021.

[6] Georgios K. Papageorgiou, Mathini Sellathurai and Yonina C. Eldar, "Deep Networks for Direction-of-Arrival Estimation in Low SNR," *IEEE Trans. Signal Process.*, vol. 69, pp. 3714-3729, 2021.

[7] A. H. El Zooghby, C. G. Christodoulou and M. Georgiopoulos, "Performance of radial-basis function networks for direction of arrival estimation with antenna arrays," *IEEE Trans. Antennas and Propag.*, vol. 45, no. 11, pp. 1611-1617, Nov. 1997.

[8] A. H. El Zooghby, C. G. Christodoulou and M. Georgiopoulos, "A neural network-based smart antenna for multiple source tracking," *IEEE Trans. Antennas and Propag.*, vol. 48, no. 5, pp. 768-776, May 2000.

[9] H. Xiang, B. Chen, T. Yang and D. Liu, "Improved De-Multipath Neural Network Models With Self-Paced Feature-to-Feature Learning for DOA Estimation in Multipath Environment," *IEEE Trans. Veh. Technol.*, vol. 69, no. 5, pp. 5068-5078, May 2020.

[10] H. M. Pour, Z. Atlasbaf and M. Hakkak, "Performance of Neural Network Trained with Genetic Algorithm for Direction of Arrival Estimation," in *Proc. IEEE 1st Mob. Comput. Wirel. Commun. Int. Conf. (MCWC)*, Amman, 2006, pp. 197-202.

[11] L. Liu et al., "Position-based modeling for wireless channel on high-speed railway under a viaduct at 2.35 GHz," *IEEE J. Sel. Areas Commun*, vol. 30, no. 4, pp. 834-845, May 2012.

[12] R. He, Z. Zhong, B. Ai and J. Ding, "An Empirical Path Loss Model and Fading Analysis for High-Speed Railway Viaduct Scenarios," *IEEE Antennas Wireless Propag. Lett.*, vol. 10, pp. 808-812, 2011.

[13] J. T. Tou and R. C. Gonzalez, Pattern Recognition Principles. Reading, MA: Addison Wesley, 1976.

[14] S. Haykin and Ed., Advances in Spectrum Analysis and Array Processing. Englewood Cliffs, NJ: Prentice-Hall, 1995, vol. III.